

Externally corrected CCSD with renormalized perturbative triples (R-ecCCSD(T)) and density matrix renormalization group and selected configuration interaction external sources

Seunghoon Lee,^{*,†} Huanchen Zhai,[†] Sandeep Sharma,^{*,‡} C. J. Umrigar,^{*,¶}
and Garnet Kin-Lic Chan^{*,†}

[†]*Division of Chemistry and Chemical Engineering, California Institute of Technology, Pasadena, California 91125, USA*

[‡]*Department of Chemistry, The University of Colorado at Boulder, Boulder, Colorado 80302, USA*

[¶]*Laboratory of Atomic and Solid State Physics, Cornell University, Ithaca, New York 14853, USA*

E-mail: slee89@caltech.edu; sandeep.sharma@colorado.edu;
cyrumrigar@gmail.com; gkc1000@gmail.com

Abstract

We investigate the renormalized perturbative triples correction together with the externally corrected coupled-cluster singles and doubles (ecCCSD) method. We take the density matrix renormalization group (DMRG) and heatbath CI (HCI) as external sources for the ecCCSD equations. The accuracy is assessed for the potential energy surfaces of H₂O, N₂, and F₂. We find that the triples correction significantly improves on ecCCSD and we do not see any instability of the renormalized triples with respect to dissociation. We explore how to

balance the cost of computing the external source amplitudes with respect to the accuracy of the subsequent CC calculation. In this context, we find that very approximate wavefunctions (and their large amplitudes) serve as an efficient and accurate external source. Finally, we characterize the domain of correlation treatable using the externally corrected method and renormalized triples combination studied in this work via a well-known wavefunction diagnostic.

1 Introduction

Electronic structure methods that can efficiently handle both static and dynamic correlation remain an important area of investigation. Because there is a wide spectrum of strongly correlated problems, ranging from mildly "quasi"-degenerate scenarios (e.g. in the electronic structure of diradicals^{1,2}) to extensively near-degenerate problems (e.g. in the electronic structure of multi-centre transition metal clusters³⁻⁵) a variety of theoretical strategies have been proposed.

For highly-degenerate problems, it is common to combine dynamic correlation methods with an explicit treatment of a multi-reference state. The representation of the multi-reference state can range from an exact complete active space (CAS) representation⁶⁻⁸ (for small numbers of orbitals), to density matrix renormalization group (DMRG)⁹⁻²³ (e.g. when almost all orbitals are degenerate), to selected configuration interaction²⁴⁻⁴⁴ and Monte Carlo approximations⁴⁵⁻⁴⁹ for intermediate cases. On top of these, various flavours of perturbation theory,⁵⁰⁻⁶² configuration interaction,⁶³⁻⁶⁶ and exponential approximations^{58,67-69} have been explored. However, the combination of dynamic correlation with multi-reference representations is not straightforward and usually leads to added conceptual, implementation, and computational complexity.

For quasi-degenerate problems, an alternative strategy can be used, which incorporates a limited amount of static correlation on top of an existing SR method. This has been particularly popular in conjunction with SR coupled cluster methods.⁷⁰⁻⁷⁵ Some examples include variants of tailored coupled cluster⁷⁶⁻⁸¹ and externally corrected coupled cluster methods.⁸²⁻⁸⁵ The computational cost of such SR static correlation methods is often lower than that of true MR dynamic correlation methods and thus large active spaces become affordable. However, the approximations are limited

to problems with only a modest amount of degeneracy.

In this work, we will focus on quasi-degenerate problems, and in particular, we will investigate the externally corrected coupled cluster method.⁸²⁻⁸⁵ This extracts static correlation from a MR method by using the MR wavefunction as an "external" source of higher order coupled cluster amplitudes. For example, in the ecCCSD approximation, the T_3 and T_4 amplitudes are extracted from the external source and a new set of T_1 and T_2 amplitudes are computed in their presence. Should the T_3 and T_4 amplitudes be exact, then the T_1 and T_2 amplitudes and the energy will be exact. A different, spiritually related, approximation is tailored CCSD,⁷⁶⁻⁷⁸ which has been of renewed interest of late.⁷⁹⁻⁸¹ Here, instead of higher order cluster amplitudes, the large (active space) T_1 and T_2 amplitudes are fixed from an external source.

The ecCCSD method has a long history and external sources, ranging from unrestricted Hartree-Fock⁸⁶⁻⁸⁹ to CASSCF and CASCI⁹⁰⁻⁹⁴ and, most recently, full configuration interaction quantum Monte Carlo,⁹⁵ have been used. One of the more successful applications of ecCCSD is the reduced multireference (RMR) CCSD method,^{96,97} which uses a MRCISD wave function as the external source. RMR CCSD(T), which incorporates some of the residual dynamic correlation through perturbative triples, has also been studied.⁹⁸ Despite the promising performance of RMRCCSD(T) in several studies,⁹⁹⁻¹⁰⁷ it suffers from two main limitations. First, conventional MRCISD can only be applied for modest sizes of active spaces (typically, up to about 16 orbitals as limited by the exact CAS treatment). Second, the (T) correction, although not divergent like its single-reference counterpart, still overcorrects the dynamical correlation in the bond-stretched region.¹⁰⁸

In this work, we make two modifications to ecCCSD to overcome and ameliorate the above limitations. First, we utilize variational DMRG and HCI wave functions as external sources for ecCCSD. This allows for the use of larger quasidegenerate active spaces, of the size typically treated by DMRG and HCI. Second, we explore the renormalized perturbative triples correction. This has been shown in the single reference setting to ameliorate the overcorrection of standard perturbative triples,¹⁰⁹ without affecting the computational scaling.

We describe the use of DMRG and HCI as external sources for ecCCSD in Section 2.1. It

is possible to create a near-exact method by using a near-exact external source. Since near-exact external sources can be computed by DMRG and HCI for the small systems we employ as test cases in this paper, the critical question is not simply the accuracy of the method, but the balance between cost and accuracy. To this end, we explore a variety of approximate treatments of the external DMRG and HCI sources as discussed in Sec. 2.2. The various triples approximations for ecCCSD are discussed in Section 2.3. Computational details are provided in Section 3 and the accuracy of the renormalized perturbative triples correction is assessed for three potential energy surfaces (PESs) in Sections 4.1-4.4. We characterize the range of quasi-degenerate correlations captured in this work in Section 4.6. Finally we discuss the limitations of this method in Section 4.7 and summarize our findings in Section 5.

2 Theory

In this work, we use a reference configuration $|\Phi\rangle$ with the same occupancy as the Hartree-Fock (HF) determinant. It is useful to define a projection operator onto the space of k -tuply excited configurations relative to the reference; we denote this Q_k . The external source is used to provide an important subset of the triply and quadruply excited configurations; the projector onto this subset is denoted Q_k^{ec} , and its complement is Q_k^c . Thus

$$Q_k = Q_k^{ec} + Q_k^c, \quad k = 3, 4, \tag{1}$$

2.1 Externally corrected CCSD with DMRG and HCI wave functions

In ecCCSD, the coupled cluster operator T is given by

$$T = T_1 + T_2 + Q_3^{ec}T_3 + Q_4^{ec}T_4. \tag{2}$$

Here, T_n , $n = 1, 2, 3, 4$, are the n -fold cluster operators. In this work, we extract $Q_k^{\text{ec}}T_k$, $k = 3, 4$ from the DMRG or the HCI variational wave function. For the DMRG wave function, the triply and quadruply excited configurations D_p that define Q_k^{ec} , $k = 3, 4$ are chosen to be those where the magnitude of the CI coefficient c_p is above a threshold, i.e.

$$|c_p| > s\sqrt{\omega}, \quad (3)$$

where s is an arbitrary scaling factor and ω is the largest discarded weight of the density matrix at the maximum bond dimension in two-dot DMRG sweeps (carried out without noise). An efficient algorithm to convert a matrix-product state to CI coefficients above a given threshold is described in Appendix A. For the HCI variational wave function, D_p is included in the projectors Q_k^{ec} , $k = 3, 4$ using the heatbath algorithm with a threshold ϵ ,⁴² i.e., it is included if

$$|\langle D_p | H | D_q \rangle c_q| > \epsilon, \quad (4)$$

for at least one determinant D_q which is already in the variational space. The extracted CI coefficients are then converted into cluster amplitudes.

The T_1 and T_2 amplitudes are obtained by solving the ecCCSD equations using fixed $Q_3^{\text{ec}}T_3$ and $Q_4^{\text{ec}}T_4$,

$$0 = (Q_1 + Q_2)(H_N e^{T_1+T_2+Q_3^{\text{ec}}T_3+Q_4^{\text{ec}}T_4})_C |\Phi\rangle, \quad (5)$$

where H_N is the Hamiltonian in normal-ordered form, and the subscript C denotes the connected part of the corresponding operator expression. With the relaxed T_1 and T_2 , the ecCCSD correlation energy of the ground state is obtained as

$$\Delta E_0^{\text{ecCCSD}} = \langle \Phi | (H_N e^{T_1+T_2+Q_3^{\text{ec}}T_3+Q_4^{\text{ec}}T_4})_C | \Phi \rangle. \quad (6)$$

2.2 Approximations in the external source

While DMRG and HCI can, in small molecules, be a source of nearly exact T_3 and T_4 amplitudes even in the full orbital space, this provides no computational advantage as such calculations are more expensive than the subsequent coupled cluster calculation. Consequently, it is important to balance the cost of the external source calculation and that of the subsequent coupled cluster calculation by making approximations in the external source. This introduces the additional complication that one must ensure that errors introduced into the external source do not lead to unacceptable errors in the final coupled cluster calculation.

In this work, we consider six different types of approximate external sources with different sizes of active spaces and different values of parameters summarized in Table 1. Type I uses CASSCF-like external sources in minimal active spaces. Since the minimal active space of F_2 , i.e., two electrons in two orbitals (2e,2o), does not contain T_3 and T_4 , we perform minimal active space ecCC calculations for only H_2O and N_2 (with (4e,4o) and (6e,6o), respectively). These provide amplitudes that are very close to the exact CASSCF amplitudes. However, these amplitudes lack the relaxation that comes from allowing excitations within a larger space of orbitals, and of course the amplitudes outside the minimal active space are completely absent. Type III uses CASCI-like external sources (the orbitals are not optimized to save computer time) in larger active spaces ((8e,18o), (10e,16o), and (14e,16o) for H_2O , N_2 , and F_2 , respectively).

In either case, one can potentially introduce bad external amplitudes if the effect of relaxation on the amplitude upon going to a larger space is large relative to the size of the amplitude (e.g. changes its sign). Thus, we study also Type II and Type IV external sources which are similar to Type I and Type II external sources respectively except that they employ an additional threshold to screen out all except the largest T_3 and T_4 amplitudes. The absolute values of the T_3 and T_4 elements at the most stretched geometry of each molecule are sorted in a single large vector. The norm of the vector is computed. Only the largest elements of the vector are retained such that the resulting norm is more than 80% of the norm of the full vector. Along PESs of each molecule, we used the same set of elements of T_3 and T_4 (but with the appropriate values for each geometry) as

the external sources, to maintain the smoothness of the PESs.

As discussed in Section 4.4, the type-III and type-IV sources improve upon the PESs obtained from the type-I and type-II sources, but the DMRG calculations to obtain the sources incur a higher computational cost than the subsequent CC calculations. To reduce the cost, we have also tried type-V sources, which employ loosely converged DMRG wave functions with small bond dimensions of $M = 25, 50$, and 100 . Finally, type-VI sources employ large thresholds $\epsilon = 0.01$, and 0.003 to obtain loosely converged HCI wave functions in the full orbital spaces. This combination has the advantage that it can be considered a black-box method wherein a single parameter ϵ controls the tradeoff between accuracy and cost.

Table 1: Six types of approximate external sources. Detailed explanation to be found in the main text.

Type	Method	Active space	Cut-off parameters	
			Wave function	Cluster amplitude
I	DMRG HCI	Minimal ^a	$M = 2000$ $\epsilon = 10^{-7}$	100% with $s = 0.1$ 100%
II	DMRG HCI	Minimal ^a	$M = 2000$ $\epsilon = 10^{-7}$	80% with $s = 0.1$ 80%
III	DMRG	Larger ^b	$M = 2000$	100% with $s = 0.1$
IV	DMRG	Larger ^b	$M = 2000$	80% with $s = 0.1$
V	DMRG	Larger ^b	$M = 25, 50, 100$	80% for H ₂ O and N ₂ , 100% for F ₂ with $s = 0.01$
VI	HCI	Full ^c	$\epsilon = 0.01, 0.003$	100%

^a(4e, 4o) for H₂O, (6e, 6o) for N₂

^b(8e, 18o) for H₂O, (10e, 16o) for N₂, (14e, 16o) for F₂

^c(10e, 58o) for H₂O, (14e, 60o) for N₂, (14e, 58o) for F₂

2.3 Perturbative triples corrections

Expressions for the standard, renormalized, and completely renormalized perturbative triples corrections can be written down in analogy with their single reference definitions.¹⁰⁹ We first define the completely renormalized (CR)-ecCCSD(T) correction. We use the state $|\Psi^{\text{ecCCSD(T)}}\rangle$ defined as

$$|\Psi^{\text{ecCCSD(T)}}\rangle = (1 + T_1 + T_2 + Q_3^{\text{ec}}T_3 + Q_3^c T_3^{[2]} + Q_3^c Z_3)|\Phi\rangle, \quad (7)$$

$$T_3^{[2]}|\Phi\rangle = R_0^{(3)}(V_N T_2)_C|\Phi\rangle, \quad (8)$$

$$Z_3|\Phi\rangle = R_0^{(3)}V_N T_1|\Phi\rangle. \quad (9)$$

where V_N is the two-body part of the Hamiltonian in normal-ordered form and $R_0^{(3)}$ denotes the three-body component of the reduced resolvent operator in many-body perturbation theory, given by differences of orbital energies in the denominator.⁷⁵ The resulting formula for the CR-ecCCSD(T) energy correction is

$$\delta_0^{\text{CR-ecCCSD(T)}} = \frac{\langle \Psi^{\text{ecCCSD(T)}} | Q_3^c (H_N e^T)_C | \Phi \rangle}{\langle \Psi^{\text{ecCCSD(T)}} | e^T | \Phi \rangle}. \quad (10)$$

The energy corrections for renormalized (R)-ecCCSD(T) and ecCCSD(T) can be obtained by taking the lowest-order estimates of the correction and by assuming the denominator to be one, i.e.,

$$\delta_0^{\text{R-ecCCSD(T)}} = \frac{\langle \Psi^{\text{ecCCSD(T)}} | Q_3^c (V_N T_2)_C | \Phi \rangle}{\langle \Psi^{\text{ecCCSD(T)}} | e^T | \Phi \rangle}, \quad (11)$$

$$\delta_0^{\text{ecCCSD(T)}} = \langle \Psi^{\text{ecCCSD(T)}} | Q_3^c (V_N T_2)_C | \Phi \rangle. \quad (12)$$

Unlike perturbative triples without external correction (as in CCSD(T)), the approximate perturbative expression $T_3^{[2]}$ is only evaluated for determinants omitted in the external source. Thus it is not expected to diverge as long as the external source includes all degeneracies. Nonetheless, it can still overestimate the triples correlation. The role of the denominator in the "renormalized" triples

approximations is to rescale this correction, which can be expected to reduce the overestimation.

3 Computational Details

All CC calculations were performed using cc-pVTZ basis sets.¹¹⁰ The ecCC calculations were performed with the six different types of external sources summarized in Table 1 and discussed in Section 2.2. The CASSCF-like external sources (type I and II) used natural orbitals in the minimal active spaces and CASSCF orbitals for the core and external spaces, while the CASCI-like external sources (type III-VI) used HF orbitals.

All CC calculations were carried out using a local version of PySCF¹¹¹ interfaced with StackBLOCK¹¹²⁻¹¹⁵ for DMRG and Arrow^{44,116,117} for HCI. We used Dice¹¹⁶⁻¹¹⁸ to get accurate SHCI PESs.

4 Numerical results

4.1 PESs with type-I external sources

The dissociation PESs of H₂O and N₂, shown in Fig. 1, were obtained by the ecCC methods using the type-I external sources in Table 1 (i.e. near exact wave functions in the minimal active spaces and all amplitudes of T_3 and T_4). As expected, the ecCC curves with tightly converged HCI and DMRG external sources are almost identical. Thus, we show the PESs of ecCC using only one of these external sources (colored solid lines) and the PESs of CC (colored dotted lines) in Fig. 1. These are compared against accurate PESs represented as black lines obtained by SHCI in the full space. The accurate energies from SHCI are given in the Supporting Information. The mean absolute errors (MAE) and the non-parallelity errors (NPE) of the PESs are listed in Table 2.

The CCSD curves (blue dotted lines) have an unphysical dip due to an inadequate treatment of static correlation. This problem is completely eliminated within ecCCSD (blue solid line). However, there are significant errors with respect to the black curve at large distances, giving a (MAE,NPE) of (24.0, 65.9) m E_H for H₂O and (64.1, 149.9) m E_H for N₂.

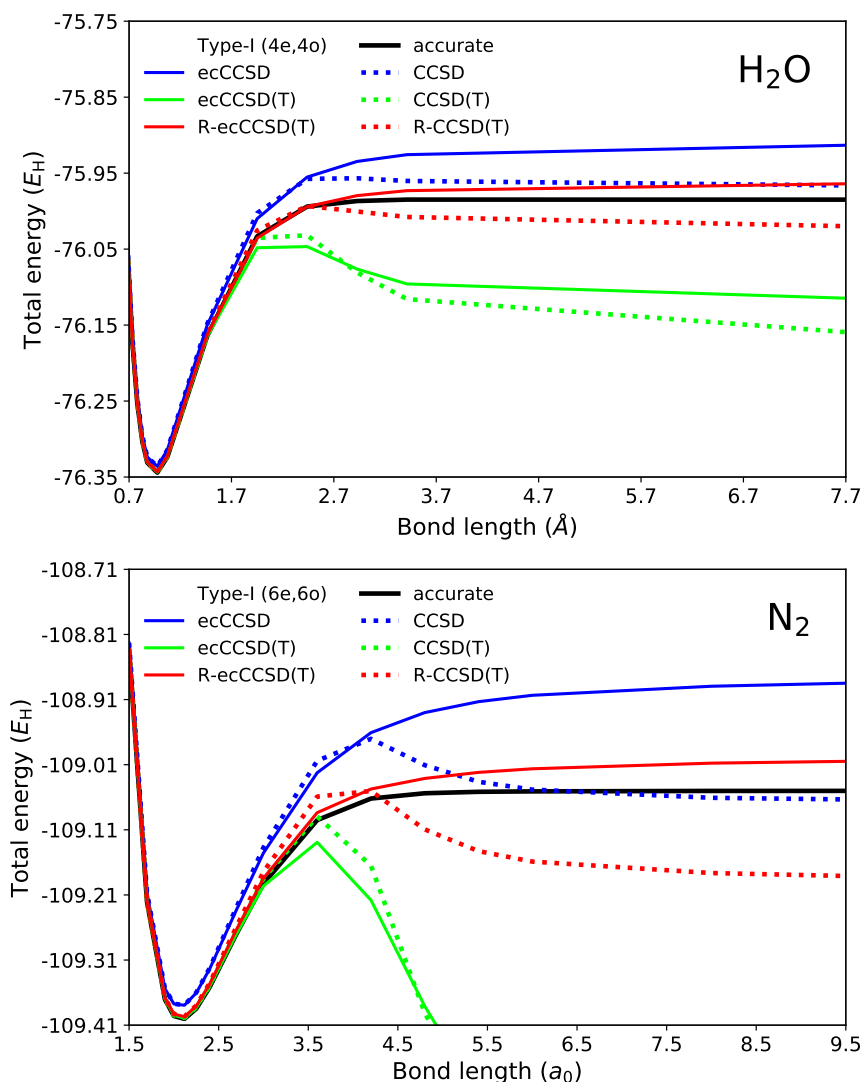
We see that the (T) correction captures much of the missing dynamic correlation, such that the green ecCCSD(T) curves reach an accuracy of $1 mE_H$ around the equilibrium geometry. However, when the bond is stretched, the (T) correction overestimates the dynamic correlation, leading to another unphysical dip in the PESs. Although this overestimation can easily be reduced by increasing the size of the active space for the small systems treated here, this would be very expensive for large systems. Alternatively, we can use the renormalized triples formula to damp the (T) correction in Eq. (11). R-ecCCSD(T) (the solid red curves) completely removes the unphysical dips in the PESs. These attain $(MAE, NPE) = (3.9, 23.1)$ and $(12.8, 41.4) mE_H$ for H_2O and N_2 , respectively.

4.2 PESs with type-II external sources

The difference between the type-I and type-II external sources is that the former use all the amplitudes of T_3 and T_4 while the latter use only a small number of the largest amplitudes, which contribute about 80% of the total weight of T_3 and T_4 (see Table 1 and Section 2.2). For the minimal active space of H_2O , i.e. (4e,4o), the external source contains only one non-zero T_4 amplitude, and all elements of T_3 are zero to within numerical noise. Thus, the PESs of ecCC using 80% of the external amplitudes (type-II) are almost identical to those using 100% of the external amplitudes (type-I). On the other hand, for the minimal active space of N_2 , i.e. (6e,6o), the external source contains several large T_3 and T_4 amplitudes. At the stretched geometry corresponding to a bond length of $10a_0$, 80% of the total T_3 and T_4 amplitude weight is recovered by the nine largest elements of T_4 . Figure 2 shows that the type-II external sources, although using fewer amplitudes, improve the PESs of ecCCSD and R-ecCCSD(T) relative to the type-I sources. The PES of R-ecCCSD(T) displays a $(MAE, NPE) = (5.4, 13.9) mE_H$.

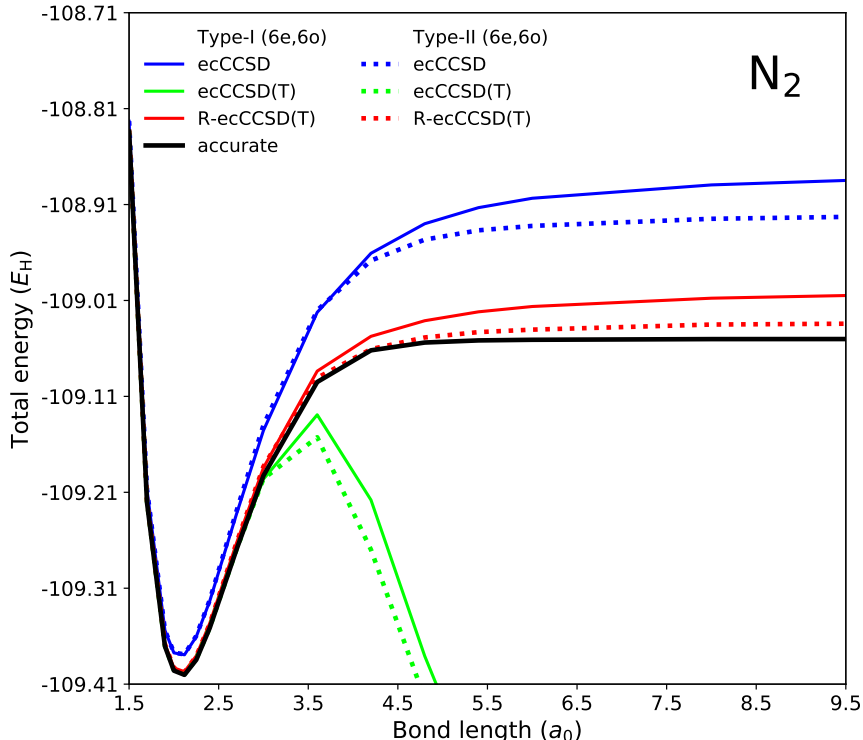
One concern with partial use of the amplitudes in the minimal active space is the possibility of divergence in (T). Assuming a HF occupation of the natural orbitals, the recomputed orbital energies (diagonal parts of the Fock matrix) of the holes and those of the particles are such that the system retains a sizable gap. N_2 at the $10.0a_0$ bond length, for example, has a gap of around

Figure 1: PESs of H_2O and N_2 in the top and bottom panels, respectively, obtained with the CC methods and the ecCC methods using the type-I external sources. The type-I sources correspond to near exact wave functions from the minimal active space, and use all the amplitudes of T_3 and T_4 . The blue, green, and red solid lines are the ecCCSD, ecCCSD(T), and R-ecCCSD(T) PESs, respectively. These are to be compared with the PESs of CC represented as dotted lines. The black lines are accurate PESs obtained by SHCI.



0.1 Hartrees between the three occupied orbitals and the three unoccupied orbitals. This prevents the divergence of the (T) and the renormalized (T) corrections at the bond lengths we considered (although (T) largely overestimates dynamic correlation).

Figure 2: PESs of N_2 obtained by the ecCC methods using all the external amplitudes (type-I) and some of the largest external amplitudes (type-II) from the minimal active space (solid and dotted lines, respectively). Other descriptions are the same as in Fig.1



4.3 PESs with type-III and type-IV external sources

In addition, we investigated PESs of R-ecCCSD(T) using larger active spaces with all amplitudes (type-III) and 80% of the amplitudes (type-IV). We used active spaces of (8e,18o), (10e,16o), and (14e,16o) for H_2O , N_2 , and F_2 , respectively, and obtained near exact wave functions in the spaces. The PESs of ecCC using the type-III and type-IV external sources are shown as colored solid and dotted lines, respectively, in Figure 3. The MAE and NPE of the PESs are given in Table 2.

For H_2O and N_2 , the resulting PESs of R-ecCCSD(T) with all amplitudes (red solid lines in the top and middle panels) achieve (MAE,NPE) = (2.9, 18.0) and (12.1, 44.3) mE_H , respectively.

These are minor improvements compared to the results using the minimal active space external sources. However, the PESs obtained using only 80% of the external amplitudes (red dotted lines) are much closer to the black, accurate PES, and reach a (MAE,NPE) = (1.1, 8.1) and (4.6, 8.4) mE_H . Similarly to in the minimal active space, 80% of the amplitude weight in the larger active space corresponds to only one element of T_4 for H_2O and the nine largest elements of T_4 for N_2 . When we can find such large elements, the partial usage of the amplitudes clearly has advantages in both accuracy and efficiency. It furthermore points to the importance of accounting for the error from missing relaxation in the external source amplitudes.

Unlike in H_2O and N_2 , there are no particularly large elements in the T_3 and T_4 amplitudes of F_2 . To truncate the amplitudes to 80% of their weight, we used the approximately 400 largest elements of T_3 and T_4 summing to 80% of the total T_3 and T_4 weights at the bond length of 5.0 Å. The red solid and dotted lines in the bottom panel of Figure 3 show the PESs of R-ecCCSD(T) using all and 80% of the amplitudes, respectively. These two PESs are very close to the accurate black curve and reach a (MAE,NPE) = (0.9, 1.4) and (1.7, 1.6) mE_H for 100% and 80% of the amplitudes, respectively. Although both are accurate, the partial use of the external source in this case (where there is not a small number of large elements) leads to slightly worse accuracy.

4.4 PESs with type-V external sources

In the previous section, we showed that the use of larger active spaces significantly improves the ecCC PESs. However, obtaining tightly converged DMRG wave functions in large active spaces requires more CPU time than the subsequent CC calculation. For example, optimizing an external wave function with 16 orbitals requires around a few minutes of CPU time for one DMRG sweep with $M = 2000$. Although a few minutes is not prohibitively large in many applications, it is large compared to the subsequent ecCC calculation which only takes tens of seconds, at least for the small molecules considered here. In addition, the fact that in some cases only a partial use of the amplitudes led to better results in the last section suggests that it is not a good use of computational time to tightly converge the external source.

Figure 3: PESs of H_2O , N_2 , and F_2 in the top, middle, and bottom panels, respectively, for the ecCC methods using the larger than minimal active spaces and the near exact external sources. The solid and dotted lines correspond to PESs obtained using all external amplitudes of T_3 and T_4 (type-III) and only the largest amplitudes of T_4 (type-IV), respectively. The descriptions are otherwise the same as those in Fig.2.

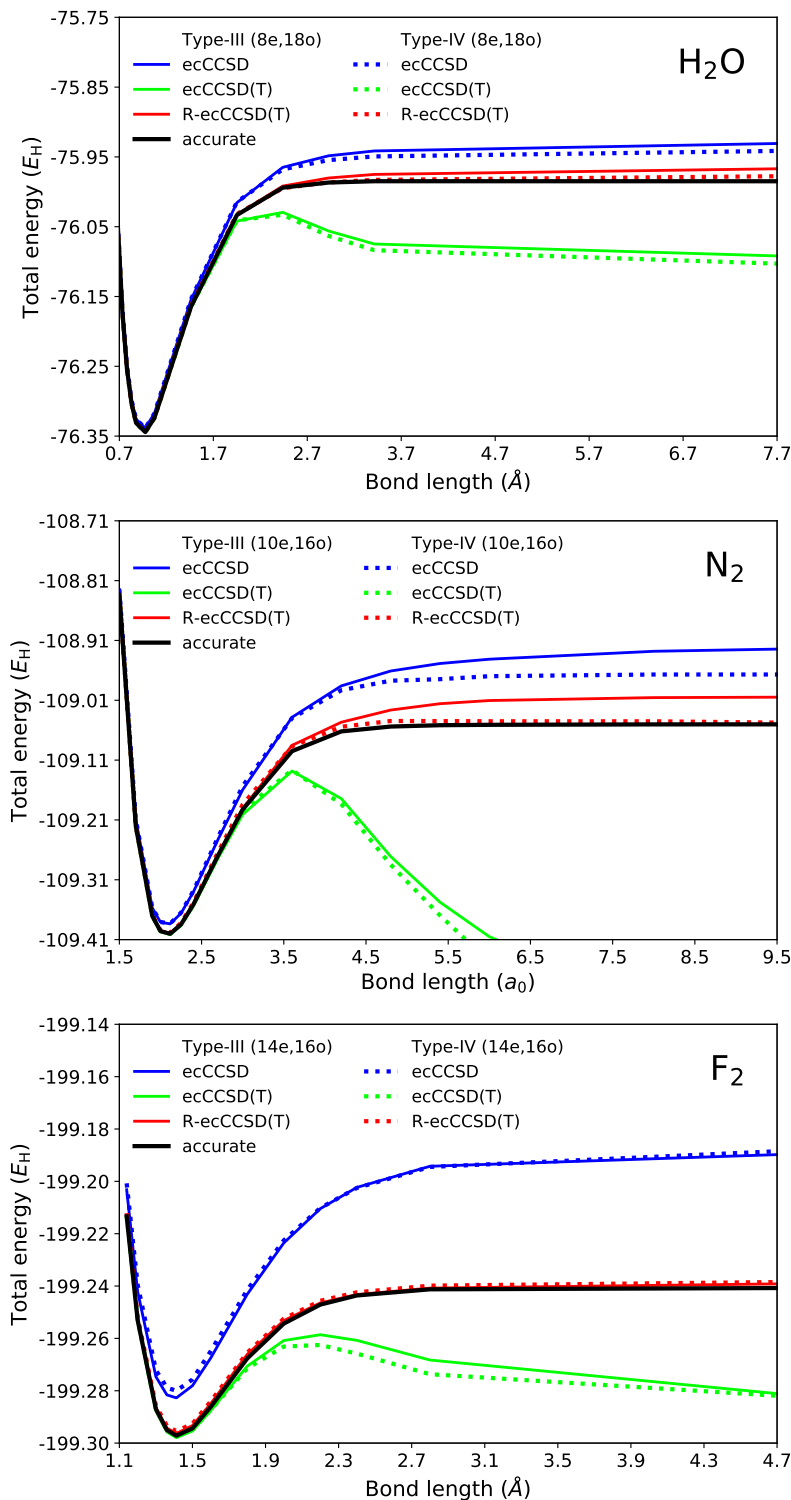


Table 2: MAE and NPE (mE_H) of H_2O , N_2 , and F_2 PESs in a range of geometries $R \in [0.68, 7.80]$ Å, $R \in [1.5, 10.0]$ a_0 , and $R \in [1.14, 5.00]$ Å, respectively. ecCC methods using the near exact external sources with all elements of T_3 and T_4 amplitudes ("100%") or only the largest elements of the T_4 amplitudes ("80%") from the external source.

Method	T_3, T_4	H_2O			N_2			F_2		
		Active	MAE	NPE	Active	MAE	NPE	Active	MAE	NPE
CCSD			15.9	30.4		32.4	102.3		34.8	57.7
ecCCSD	100%	4e,4o	24.0	65.9	6e,6o	64.1	149.9	2e,2o	a	a
	80%		24.0	65.9		57.5	114.5			
	100%	8e,18o	17.6	49.9	10e,16o	48.4	113.0	14e,16o	25.2	41.4
	80%		15.6	39.4		41.4	74.0		27.0	40.9
R-CCSD(T)			6.8	43.0		32.1	162.1		6.2	10.6
R-ecCCSD(T)	100%	4e,4o	3.9	23.1	6e,6o	12.8	41.4	2e,2o	a	a
	80%		3.9	23.1		5.4	13.9			
	100%	8e,18o	2.9	18.0	10e,16o	12.1	44.3	14e,16o	0.9	1.4
	80%		1.1	8.1		4.6	8.4		1.7	1.6

^a no T_3 and T_4 in the minimal active space of F_2

We thus now consider loosely converged DMRG sources (type-V) in the larger active spaces. We re-computed PESs of R-ecCCSD(T) shown in Figure 3 using a DMRG source with bond dimensions 25, 50, and 100. We used the truncation to 80% amplitude weight for H_2O and N_2 , while we used all the external amplitudes for F_2 . Table 3 shows the corresponding MAE and NPE in the same range of geometries in Table 2.

For all cases, when we reduced the bond dimension to $M = 100$, the MAE increased by $0.1 \sim 0.5 mE_H$, and the NPE increased by $0.3 \sim 1.0 mE_H$, compared to using $M = 2000$. However for $M = 100$, one DMRG sweep with 16 orbitals took only a few seconds of CPU time at the $10a_0$ bond length of N_2 , giving a better computational balance between the DMRG calculation and the subsequent ecCC calculations. When we further reduced the bond dimension to $M = 25$, the MAE increased by $0.9 mE_H$ and the NPE increased by 0.6 and $2.7 mE_H$ for H_2O and N_2 . In the case of F_2 , which does not have a small number of large T_3 and T_4 elements, the MAE and NPE increased more, by 3.4 and $5.4 mE_H$.

4.5 PESs with type-VI external sources

Type VI sources use the full orbital space and employ the single HCI parameter, ϵ , to select the large T_3 and T_4 amplitudes. They do not require a choice for the CAS space, and we did not further threshold the T_3 and T_4 amplitudes. However, for systems where the molecule has a low-spin ground state, but the dissociated fragments have high-spin ground states, the HCI wave functions at stretched geometries are strongly spin-contaminated when ϵ is large, even when time-reversal symmetry is employed to reduce the spin contamination. (This type of spin-contamination is avoided in the small bond dimension DMRG calculations via the full use of spin symmetry). Although this has little effect on the HCI energy, it makes the amplitudes unsuitable for ecCC calculations.

In the second part of Table 3 the MAE and NPE from type-VI sources using $\epsilon = 0.01$ and 0.003 are shown. These are evaluated over a smaller range of geometries than those used in the first part of Table 3 for the reason mentioned above. Since N_2 is a singlet that dissociates into atoms that are quartets, it has particularly large errors. The errors improve upon going from $\epsilon = 0.01$ to $\epsilon = 0.003$, in particular the PEC has an unphysical dip at $\epsilon = 0.01$ which disappears at $\epsilon = 0.003$, but the errors are still substantial. Similarly to how using all the amplitudes could lead to larger errors than only using some of the amplitudes in the previous sections, the errors incurred from the type VI sources here emphasize that the quality of the external amplitudes cannot be judged solely from the energy obtained by the external method.

4.6 Error analysis

In this section, we present the errors of R-ecCCSD(T) for the systems in this work and analyze them using the well known CC error diagnostic D_2 , defined by the matrix 2-norm of the T_2 amplitudes.¹¹⁹ The magnitude of D_2 can be used to distinguish between the SR and MR character of the different geometries on the PESs. Organic molecules are sometimes considered to have MR character when D_2 is larger than 0.18.¹¹⁹ Figure 4 shows the absolute errors on a log scale versus the D_2 diagnostic. Each symbol represents a geometry on the PESs of one of the molecules, H_2O ,

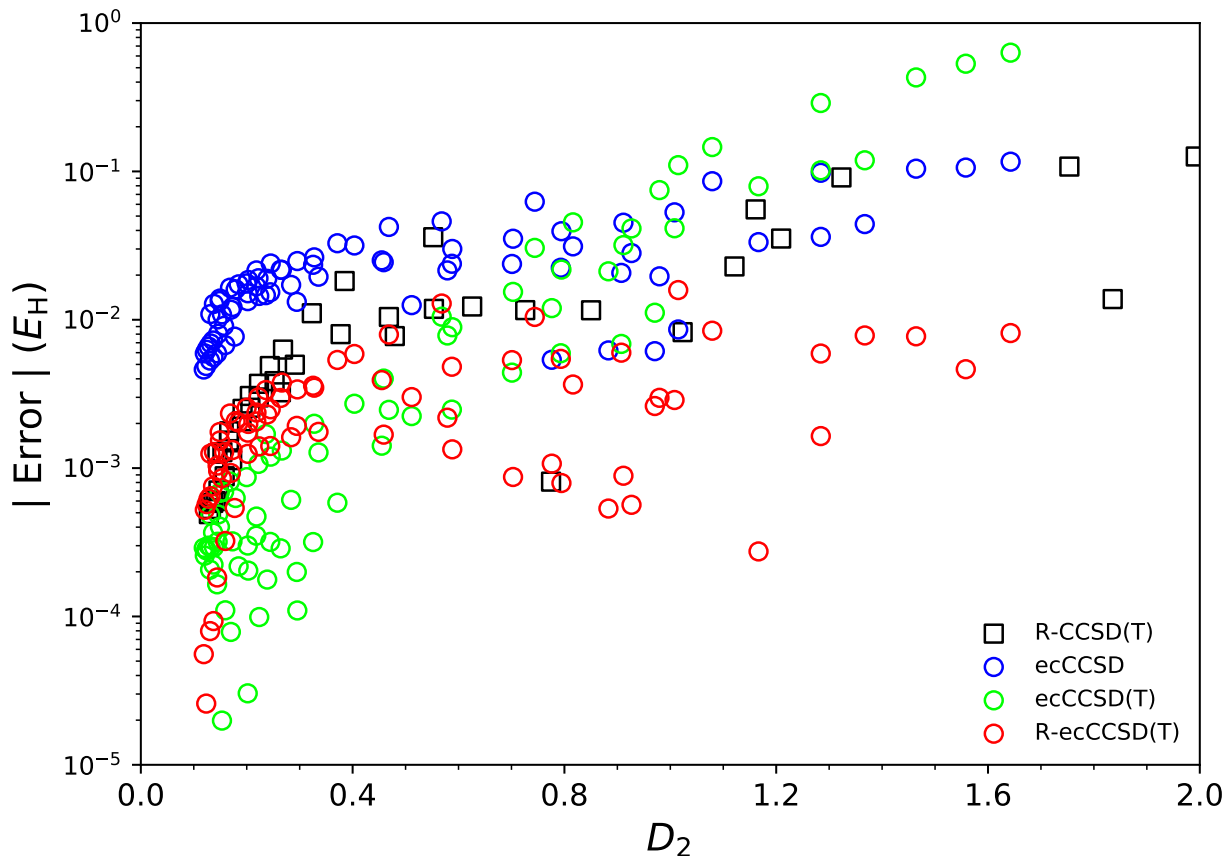
Table 3: MAE and NPE (mE_H) of R-ecCCSD(T) PESs for H_2O , N_2 , and F_2 using the approximate DMRG and HCI sources with a small bond dimension (M) or large threshold (ϵ). Detailed explanation to be found in the main text.

M	H_2O			N_2			F_2		
	Active	MAE ^a	NPE ^a	Active	MAE ^a	NPE ^a	Active	MAE ^a	NPE ^a
25		3.8	8.7		5.5	11.1		4.3	6.8
50	(8e,18o)	3.4	8.2	(10e,16o)	5.2	9.6	(14e,16o)	3.5	3.4
100		3.0	8.4		4.9	9.4		1.4	2.1
2000		2.9	8.1		4.6	8.4		0.9	1.4
ϵ	H_2O			N_2			F_2		
	Active	MAE ^b	NPE ^b	Active	MAE ^b	NPE ^b	Active	MAE ^b	NPE ^b
0.01	(10e,58o)	1.6	7.1	(14e,60o)	8.1	61.5	(14e,58o)	3.6	4.7
0.003		1.3	4.4		3.6	15.8		3.0	5.8

^a $R \in [0.68, 7.80] \text{ \AA}$, $[1.5, 10.0] a_0$, and $[1.14, 5.00] \text{ \AA}$ for H_2O , N_2 , and F_2 PESs, respectively.

^b $R \in [0.68, 3.41] \text{ \AA}$, $[1.5, 5.4] a_0$, and $[1.14, 2.80] \text{ \AA}$ for H_2O , N_2 , and F_2 PESs, respectively.

Figure 4: Absolute errors of R-CCSD(T) and ecCC methods on a log scale plotted against the D_2 diagnostic. Detailed explanation in the main text.



N_2 , and F_2 . Square symbols denote R-CCSD(T) and circle symbols denote the various externally corrected theories, using the type-V and the type-VI external sources. For D_2 ranging from 0 to 1.7, the absolute errors of R-ecCCSD(T) (red circles) are less than $0.015 E_H$ and most of the errors are smaller than those of R-CCSD(T) (black squares) and ecCCSD (blue circles). The absolute errors of R-ecCCSD(T) are less than those of ecCCSD(T) (green circles) in the MR region where $D_2 > 0.4$, while they are mostly greater than those of ecCCSD(T) in the range $0.0 < D_2 < 0.4$. Overall, it is clear to see that R-ecCCSD(T) offers the most balanced treatment of errors across a wide range of SR and MR character. However, for very weakly correlated systems, the original (T) correction is slightly more accurate than the renormalized (T) correction.

4.7 Limitations

Although the work above shows that it is possible to obtain quantitative accuracy across the full potential energy surface, at a reasonable computational cost, using the combination of external sources and the renormalized (T) correction, SR ecCC approaches have a fundamental limitation when the CI coefficient of the reference configuration (the HF configuration in this work) in the external source is exactly or numerically zero. This leads to overflow due to the assumption of intermediate normalization. The smallest reference coefficient value we encountered in this work was 0.2 at the stretched $10a_0$ geometry of N_2 . Although this coefficient is not numerically zero, it is difficult to converge the ecCCSD energy. We extracted initial amplitudes of T_1 and T_2 from the external source and then iteratively converged the ecCCSD energy using a damping parameter of 0.05 to update the amplitudes. (We did not use the direct inversion in the iterative subspace (DIIS) algorithm). At this geometry, the energy could be converged monotonically up to a threshold of 10^{-5} Hartrees, although the norm of the amplitudes could not be converged, and we simply used amplitudes from the last iteration in the set of monotonically decreasing energies.

5 Conclusion

In this work, we explored externally corrected coupled cluster with a renormalized triples correction (R-ecCCSD(T)) using DMRG and HCI and external sources. The critical question is how to best balance the accuracy and cost of computing the external source with the cost of the overall method. To this end, we considered multiple types of external sources: "exact" external sources, where the DMRG and HCI wavefunctions were tightly converged, and "approximate" external sources where they were loosely converged. We also considered both "full" usage of the T_3 and T_4 amplitudes, and "partial" usage, wherein we retained only the largest elements.

For all systems considered here, we found that R-ecCCSD(T) can significantly improve on the description of the potential energy surface given either by the external source alone or CC alone. For example, the unphysical dips in the PES of H_2O and N_2 in the bond-stretched region can be completely eliminated. The use of approximate external sources, possibly with truncation to only the large T_3 and T_4 amplitudes, appears to be a practical way to balance the cost of the external calculation and the coupled cluster calculation in small molecules. Using the D_2 diagnostic to characterize the different points on the potential energy surfaces, we find that R-ecCCSD(T) gives absolute errors of less than $15 mE_H$ in the range of D_2 from 0.0 to 1.7. In fact, the errors of R-ecCCSD(T) are less than those of ecCCSD and R-CCSD(T) in almost all cases, except when D_2 is very small, where the renormalized (T) correction appears to be slightly less accurate than the simple (T) correction.

There are several interesting questions remaining which lie beyond what we have considered in this work. For example, while R-ecCCSD(T) appears quite stable up to large values of the D_2 diagnostic, what is the largest amount of multi-reference character which can be handled? Here, the difficulty in solving the CC equations, and the divergence of the amplitudes reflecting the problems of intermediate normalization, cannot be ignored. In addition, in the realm of quasidegenerate problems, we can ask whether other non-iterative corrections such as the "completely renormalized" triples and quadruples corrections,¹⁰⁹ corresponding to CR-ecCCSD(T) and CR-ecCCSD(T,Q), would further improve on the present R-ecCCSD(T) method. Finally, the current approximation,

with its modest computational requirements on the external source, is applicable to the same scale of systems that can be handled by single reference coupled cluster methods. Thus understanding the performance of this method in larger correlated systems is of interest.

Note: As this work was being prepared for submission, we were made aware of a related recent submission to the arxiv,¹²⁰ that also discusses selected configuration interaction as an external source and perturbative triples corrections in the context of externally corrected coupled cluster methods.

Acknowledgement

Work by SL, HZ and GKC was supported by the US National Science Foundation via Award CHE-1655333. GKC is a Simons Investigator. SS was supported by the US National Science Foundation grant CHE-1800584 and the Sloan research fellowship. CJU was supported in part by the AFOSR under grant FA9550-18-1-0095.

Supporting Information Available

References

- (1) Abe, M. Diradicals. *Chem. Rev.* **2013**, *113*, 7011–7088.
- (2) Nakano, M. Electronic Structure of Open-Shell Singlet Molecules: Diradical Character Viewpoint. *Top. Curr. Chem.* **2017**, *375*.
- (3) Kurashige, Y.; Chan, G. K.-L.; Yanai, T. Entangled quantum electronic wavefunctions of the Mn 4 CaO 5 cluster in photosystem II. *Nature chemistry* **2013**, *5*, 660–666.
- (4) Sharma, S.; Sivalingam, K.; Neese, F.; Chan, G. K.-L. Low-energy spectrum of iron–sulfur clusters directly from many-particle quantum mechanics. *Nat. Chem.* **2014**, *6*, 927–933.
- (5) Li, Z.; Guo, S.; Sun, Q.; Chan, G. K.-L. Electronic landscape of the P-cluster of nitrogenase as revealed through many-electron quantum wavefunction simulations. *Nat. Chem.* **2019**, *11*, 1026–1033.
- (6) Das, G.; Wahl, A. C. New Techniques for the Computation of Multiconfiguration Self-Consistent Field (MCSCF) Wavefunctions. *The Journal of Chemical Physics* **1972**, *56*, 1769–1775.
- (7) Werner, H.-J.; Meyer, W. A quadratically convergent multiconfiguration–self-consistent field method with simultaneous optimization of orbitals and CI coefficients. *The Journal of Chemical Physics* **1980**, *73*, 2342–2356.
- (8) Werner, H.-J.; Knowles, P. J. A second order multiconfiguration SCF procedure with optimum convergence. *The Journal of chemical physics* **1985**, *82*, 5053–5063.
- (9) White, S. R.; Noack, R. M. Real-space quantum renormalization groups. *Physical review letters* **1992**, *68*, 3487.
- (10) White, S. R. Density matrix formulation for quantum renormalization groups. *Physical review letters* **1992**, *69*, 2863.

- (11) White, S. R. Density-matrix algorithms for quantum renormalization groups. *Physical Review B* **1993**, *48*, 10345.
- (12) White, S. R.; Martin, R. L. Ab initio quantum chemistry using the density matrix renormalization group. *The Journal of chemical physics* **1999**, *110*, 4127–4130.
- (13) Chan, G. K.-L.; Head-Gordon, M. Highly correlated calculations with a polynomial cost algorithm: A study of the density matrix renormalization group. *The Journal of chemical physics* **2002**, *116*, 4462–4476.
- (14) Legeza, Ö.; Röder, J.; Hess, B. Controlling the accuracy of the density-matrix renormalization-group method: The dynamical block state selection approach. *Physical Review B* **2003**, *67*, 125114.
- (15) Chan, G. K.-L. An algorithm for large scale density matrix renormalization group calculations. *The Journal of chemical physics* **2004**, *120*, 3172–3178.
- (16) Legeza, Ö.; Noack, R.; Sólyom, J.; Tincani, L. *Computational Many-Particle Physics*; Springer, 2008; Vol. 739.
- (17) Chan, G.; Zgid, D. The Density Matrix Renormalization Group in Quantum Chemistry, *Annu. Rep. Comput. Chem* **2009**, *5*, 149–162.
- (18) Marti, K. H.; Reiher, M. The density matrix renormalization group algorithm in quantum chemistry. *Zeitschrift für Physikalische Chemie* **2010**, *224*, 583–599.
- (19) Chan, G. K.-L.; Sharma, S. The density matrix renormalization group in quantum chemistry. *Annual review of physical chemistry* **2011**, *62*, 465–481.
- (20) Sharma, S.; Chan, G. K.-L. Spin-adapted density matrix renormalization group algorithms for quantum chemistry. *The Journal of chemical physics* **2012**, *136*, 124121.
- (21) Wouters, S.; Van Neck, D. The density matrix renormalization group for ab initio quantum chemistry. *The European Physical Journal D* **2014**, *68*, 1–20.

- (22) Szalay, S.; Pfeffer, M.; Murg, V.; Barcza, G.; Verstraete, F.; Schneider, R.; Legeza, Ö. Tensor product methods and entanglement optimization for ab initio quantum chemistry. *International Journal of Quantum Chemistry* **2015**, *115*, 1342.
- (23) Yanai, T.; Kurashige, Y.; Mizukami, W.; Chalupský, J.; Lan, T. N.; Saitow, M. Density matrix renormalization group for ab initio Calculations and associated dynamic correlation methods: A review of theory and applications. *International Journal of Quantum Chemistry* **2015**, *115*, 283–299.
- (24) Ivanić, J.; Ruedenberg, K. Identification of deadwood in configuration spaces through general direct configuration interaction. *Theoretical Chemistry Accounts* **2001**, *106*, 339–351.
- (25) Huron, B.; Malrieu, J.; Rancurel, P. Iterative perturbation calculations of ground and excited state energies from multiconfigurational zeroth-order wavefunctions. *The Journal of Chemical Physics* **1973**, *58*, 5745–5759.
- (26) Garniron, Y.; Scemama, A.; Giner, E.; Caffarel, M.; Loos, P.-F. Selected configuration interaction dressed by perturbation. *J. Chem. Phys.* **2018**, *149*, 064103.
- (27) Loos, P.-F.; Scemama, A.; Blondel, A.; Garniron, Y.; Caffarel, M.; Jacquemin, D. A Mountaineering Strategy to Excited States: Highly Accurate Reference Energies and Benchmarks. *J. Chem. Theory Comput.* **2018**, *14*, 4360–4379.
- (28) Garniron, Y.; Scemama, A.; Loos, P.-F.; Caffarel, M. Hybrid stochastic-deterministic calculation of the second-order perturbative contribution of multireference perturbation theory. *J. Chem. Phys.* **2017**, *147*.
- (29) Buenker, R. J.; Peyerimhoff, S. D. Individualized configuration selection in CI calculations with subsequent energy extrapolation. *Theoretica chimica acta* **1974**, *35*, 33–58.

- (30) Evangelisti, S.; Daudey, J.-P.; Malrieu, J.-P. Convergence of an improved CIPSI algorithm. *Chemical Physics* **1983**, *75*, 91–102.
- (31) Harrison, R. J. Approximating full configuration interaction with selected configuration interaction and perturbation theory. *The Journal of chemical physics* **1991**, *94*, 5021–5031.
- (32) Steiner, M.; Wenzel, W.; Wilson, K.; Wilkins, J. The efficient treatment of higher excitations in CI calculations: A comparison of exact and approximate results. *Chemical Physics Letters* **1994**, *231*, 263 – 268.
- (33) Neese, F. A spectroscopy oriented configuration interaction procedure. *The Journal of Chemical Physics* **2003**, *119*, 9428–9443.
- (34) Abrams, M. L.; Sherrill, C. D. Important configurations in configuration interaction and coupled-cluster wave functions. *Chemical Physics Letters* **2005**, *412*, 121 – 124.
- (35) Bytautas, L.; Ruedenberg, K. A priori identification of configurational deadwood. *Chemical Physics* **2009**, *356*, 64 – 75, Moving Frontiers in Quantum Chemistry:.
- (36) Evangelista, F. A. A driven similarity renormalization group approach to quantum many-body problems. *The Journal of chemical physics* **2014**, *141*, 054109.
- (37) Knowles, P. J. Compressive sampling in configuration interaction wavefunctions. *Molecular Physics* **2015**, *113*, 1655–1660.
- (38) Schriber, J. B.; Evangelista, F. A. Communication: An adaptive configuration interaction approach for strongly correlated electrons with tunable accuracy. *The Journal of Chemical Physics* **2016**, *144*, 161106.
- (39) Tubman, N. M.; Lee, J.; Takeshita, T. Y.; Head-Gordon, M.; Whaley, K. B. A deterministic alternative to the full configuration interaction quantum Monte Carlo method. *The Journal of chemical physics* **2016**, *145*, 044112.

- (40) Liu, W.; Hoffmann, M. R. iCI: Iterative CI toward full CI. *Journal of chemical theory and computation* **2016**, *12*, 1169–1178.
- (41) Caffarel, M.; Applencourt, T.; Giner, E.; Scemama, A. *Recent Progress in Quantum Monte Carlo*; ACS Publications, 2016; pp 15–46.
- (42) Holmes, A. A.; Tubman, N. M.; Umrigar, C. J. Heat-Bath Configuration Interaction: An Efficient Selected Configuration Interaction Algorithm Inspired by Heat-Bath Sampling. *J. Chem. Theory Comput.* **2016**, *12*, 3674–3680.
- (43) Sharma, S.; Holmes, A. A.; Jeanmairet, G.; Alavi, A.; Umrigar, C. J. Semistochastic Heat-Bath Configuration Interaction Method: Selected Configuration Interaction with Semistochastic Perturbation Theory. *Journal of Chemical Theory and Computation* **2017**, *13*, 1595–1604.
- (44) Li, J.; Otten, M.; Holmes, A. A.; Sharma, S.; Umrigar, C. J. Fast Semistochastic Heat-Bath Configuration Interaction. *J. Chem. Phys.* **2018**, *148*, 214110.
- (45) Booth, G. H.; Thom, A. J.; Alavi, A. Fermion Monte Carlo without fixed nodes: A game of life, death, and annihilation in Slater determinant space. *The Journal of chemical physics* **2009**, *131*, 054106.
- (46) Cleland, D.; Booth, G. H.; Alavi, A. Communications: Survival of the fittest: Accelerating convergence in full configuration-interaction quantum Monte Carlo. 2010.
- (47) Ghanem, K.; Lozovoi, A. Y.; Alavi, A. Unbiasing the initiator approximation in full configuration interaction quantum Monte Carlo. *The Journal of chemical physics* **2019**, *151*, 224108.
- (48) Sabzevari, I.; Sharma, S. Improved speed and scaling in orbital space variational Monte Carlo. *Journal of chemical theory and computation* **2018**, *14*, 6276–6286.

- (49) Neuscamman, E. Subtractive manufacturing with geminal powers: making good use of a bad wave function. *Molecular Physics* **2016**, *114*, 577–583.
- (50) Andersson, K.; Malmqvist, P. A.; Roos, B. O.; Sadlej, A. J.; Wolinski, K. Second-order perturbation theory with a CASSCF reference function. *Journal of Physical Chemistry* **1990**, *94*, 5483–5488.
- (51) Angeli, C.; Cimiraglia, R.; Evangelisti, S.; Leininger, T.; Malrieu, J.-P. Introduction of n-electron valence states for multireference perturbation theory. *The Journal of Chemical Physics* **2001**, *114*, 10252–10264.
- (52) Angeli, C.; Cimiraglia, R.; Malrieu, J.-P. N-electron valence state perturbation theory: a fast implementation of the strongly contracted variant. *Chemical physics letters* **2001**, *350*, 297–305.
- (53) Angeli, C.; Cimiraglia, R.; Malrieu, J.-P. n-electron valence state perturbation theory: A spinless formulation and an efficient implementation of the strongly contracted and of the partially contracted variants. *The Journal of chemical physics* **2002**, *117*, 9138–9153.
- (54) Neuscamman, E.; Yanai, T.; Chan, G. K.-L. A review of canonical transformation theory. *International Reviews in Physical Chemistry* **2010**, *29*, 231–271.
- (55) Yanai, T.; Kurashige, Y.; Neuscamman, E.; Chan, G. K.-L. Multireference quantum chemistry through a joint density matrix renormalization group and canonical transformation theory. *The Journal of chemical physics* **2010**, *132*, 024105.
- (56) Kurashige, Y.; Yanai, T. Second-order perturbation theory with a density matrix renormalization group self-consistent field reference function: Theory and application to the study of chromium dimer. *The Journal of chemical physics* **2011**, *135*, 094104.
- (57) Sharma, S.; Chan, G. K.-L. Communication: A flexible multi-reference perturbation theory by minimizing the Hylleraas functional with matrix product states. 2014.

- (58) Sharma, S.; Alavi, A. Multireference linearized coupled cluster theory for strongly correlated systems using matrix product states. *The Journal of chemical physics* **2015**, *143*, 102815.
- (59) Guo, S.; Watson, M. A.; Hu, W.; Sun, Q.; Chan, G. K.-L. N-electron valence state perturbation theory based on a density matrix renormalization group reference function, with applications to the chromium dimer and a trimer model of poly (p-phenylenevinylene). *Journal of chemical theory and computation* **2016**, *12*, 1583–1591.
- (60) Sokolov, A. Y.; Guo, S.; Ronca, E.; Chan, G. K.-L. Time-dependent N-electron valence perturbation theory with matrix product state reference wavefunctions for large active spaces and basis sets: Applications to the chromium dimer and all-trans polyenes. *The Journal of chemical physics* **2017**, *146*, 244102.
- (61) Sharma, S.; Holmes, A. A.; Jeanmairet, G.; Alavi, A.; Umrigar, C. J. Semistochastic heat-bath configuration interaction method: Selected configuration interaction with semistochastic perturbation theory. *Journal of chemical theory and computation* **2017**, *13*, 1595–1604.
- (62) Guo, S.; Li, Z.; Chan, G. K.-L. Communication: An efficient stochastic algorithm for the perturbative density matrix renormalization group in large active spaces. *The Journal of chemical physics* **2018**, *148*, 221104.
- (63) Lischka, H.; Shepard, R.; Brown, F. B.; Shavitt, I. New implementation of the graphical unitary group approach for multireference direct configuration interaction calculations. *International Journal of Quantum Chemistry* **1981**, *20*, 91–100.
- (64) Szalay, P. G.; Muller, T.; Gidofalvi, G.; Lischka, H.; Shepard, R. Multiconfiguration self-consistent field and multireference configuration interaction methods and applications. *Chemical reviews* **2012**, *112*, 108–181.

- (65) Lischka, H.; Shepard, R.; Pitzer, R. M.; Shavitt, I.; Dallos, M.; Müller, T.; Szalay, P. G.; Seth, M.; Kedziora, G. S.; Yabushita, S., et al. High-level multireference methods in the quantum-chemistry program system COLUMBUS: Analytic MR-CISD and MR-AQCC gradients and MR-AQCC-LRT for excited states, GUGA spin-orbit CI and parallel CI density. *Physical Chemistry Chemical Physics* **2001**, *3*, 664–673.
- (66) Saitow, M.; Kurashige, Y.; Yanai, T. Fully internally contracted multireference configuration interaction theory using density matrix renormalization group: A reduced-scaling implementation derived by computer-aided tensor factorization. *Journal of chemical theory and computation* **2015**, *11*, 5120–5131.
- (67) Paldus, J.; Li, X. *Adv. Chem. Phys.* **1999**, 1–175.
- (68) Kong, L.; Shamasundar, K.; Demel, O.; Nooijen, M. State specific equation of motion coupled cluster method in general active space. *The Journal of chemical physics* **2009**, *130*, 114101.
- (69) Jeziorski, B. Multireference coupled-cluster Ansatz. *Molecular Physics* **2010**, *108*, 3043–3054.
- (70) Čížek, J. On the correlation problem in atomic and molecular systems. Calculation of wavefunction components in Ursell-type expansion using quantum-field theoretical methods. *The Journal of Chemical Physics* **1966**, *45*, 4256–4266.
- (71) Čížek, J. On the use of the cluster expansion and the technique of diagrams in calculations of correlation effects in atoms and molecules. *Advances in chemical physics* **1969**, 35–89.
- (72) Čížek, J.; Paldus, J. Correlation problems in atomic and molecular systems III. Rederivation of the coupled-pair many-electron theory using the traditional quantum chemical methodst. *International Journal of Quantum Chemistry* **1971**, *5*, 359–379.

- (73) Paldus, J.; Čížek, J.; Shavitt, I. Correlation Problems in Atomic and Molecular Systems. IV. Extended Coupled-Pair Many-Electron Theory and Its Application to the B H 3 Molecule. *Physical Review A* **1972**, *5*, 50.
- (74) Bartlett, R. J. In *Modern Electronic Structure Theory*; Yarkony, D. R., Ed.; World Scientific, 1995; Vol. 1; pp 1047–1131.
- (75) Shavitt, I.; Bartlett, R. J. *Many-body methods in chemistry and physics: MBPT and coupled-cluster theory*; Cambridge university press, 2009.
- (76) Kinoshita, T.; Hino, O.; Bartlett, R. J. Coupled-cluster method tailored by configuration interaction. *The Journal of chemical physics* **2005**, *123*, 074106.
- (77) Hino, O.; Kinoshita, T.; Chan, G. K.-L.; Bartlett, R. J. Tailored coupled cluster singles and doubles method applied to calculations on molecular structure and harmonic vibrational frequencies of ozone. *The Journal of chemical physics* **2006**, *124*, 114311.
- (78) Lyakh, D. I.; Lotrich, V. F.; Bartlett, R. J. The ‘tailored’CCSD (T) description of the automerization of cyclobutadiene. *Chemical Physics Letters* **2011**, *501*, 166–171.
- (79) Veis, L.; Antalík, A.; Brabec, J.; Neese, F.; Legeza, O.; Pittner, J. Coupled cluster method with single and double excitations tailored by matrix product state wave functions. *The journal of physical chemistry letters* **2016**, *7*, 4072–4078.
- (80) Faulstich, F. M.; Máté, M.; Laestadius, A.; Csirik, M. A.; Veis, L.; Antalík, A.; Brabec, J.; Schneider, R.; Pittner, J.; Kvaal, S., et al. Numerical and theoretical aspects of the DMRG-TCC method exemplified by the nitrogen dimer. *Journal of chemical theory and computation* **2019**, *15*, 2206–2220.
- (81) Vitale, E.; Alavi, A.; Kats, D. FCIQMC-tailored distinguishable cluster approach. *Journal of Chemical Theory and Computation* **2020**, *16*, 5621–5634.

- (82) Paldus, J.; Planelles, J. Valence bond corrected single reference coupled cluster approach. *Theoretica chimica acta* **1994**, *89*, 13–31.
- (83) Planelles, J.; Paldus, J.; Li, X. Valence bond corrected single reference coupled cluster approach. *Theoretica chimica acta* **1994**, *89*, 33.
- (84) Planelles, J.; Paldus, J.; Li, X. Valence bond corrected single reference coupled cluster approach. *Theoretica chimica acta* **1994**, *89*, 59.
- (85) Paldus, J. Externally and internally corrected coupled cluster approaches: an overview. *Journal of Mathematical Chemistry* **2017**, *55*, 477–502.
- (86) Paldus, J.; Boyle, M. Cluster analysis of the full configuration interaction wave functions of cyclic polyene models. *International Journal of Quantum Chemistry* **1982**, *22*, 1281–1305.
- (87) Paldus, J.; Chin, E.; Grey, M. Bond length alternation in cyclic polyenes. II. Unrestricted hartree–fock method. *International journal of quantum chemistry* **1983**, *24*, 395–409.
- (88) Paldus, J.; Čížek, J.; Takahashi, M. Approximate account of the connected quadruply excited clusters in the coupled-pair many-electron theory. *Physical Review A* **1984**, *30*, 2193.
- (89) Piecuch, P.; Tobol, R.; Paldus, J. Approximate account of connected quadruply excited clusters in single-reference coupled-cluster theory via cluster analysis of the projected unrestricted Hartree-Fock wave function. *Physical Review A* **1996**, *54*, 1210.
- (90) Peris, G.; Planelles, J.; Paldus, J. Single-reference CCSD approach employing three-and four-body CAS SCF corrections: A preliminary study of a simple model. *International journal of quantum chemistry* **1997**, *62*, 137–151.
- (91) Li, X.; Peris, G.; Planelles, J.; Rajadall, F.; Paldus, J. Externally corrected singles and doubles coupled cluster methods for open-shell systems. *The Journal of chemical physics* **1997**, *107*, 90–98.

- (92) Peris, G.; Rajadell, F.; Li, X.; Planelles, J.; Paldus, J. Externally corrected singles and doubles coupled cluster methods for open-shell systems. II. Applications to the low lying doublet states of OH, NH₂, CH₃ and CN radicals. *Molecular Physics* **1998**, *94*, 235–248.
- (93) Stolarczyk, L. Z. Complete active space coupled-cluster method. Extension of single-reference coupled-cluster method using the CASSCF wavefunction. *Chemical physics letters* **1994**, *217*, 1–6.
- (94) Xu, E.; Li, S. The externally corrected coupled cluster approach with four-and five-body clusters from the CASSCF wave function. *The Journal of chemical physics* **2015**, *142*, 094119.
- (95) Deustua, J. E.; Magoulas, I.; Shen, J.; Piecuch, P. Communication: Approaching exact quantum chemistry by cluster analysis of full configuration interaction quantum Monte Carlo wave functions. *The Journal of Chemical Physics* **2018**, *149*, 151101.
- (96) Li, X.; Paldus, J. Reduced multireference CCSD method: An effective approach to quasidegenerate states. *The Journal of Chemical Physics* **1997**, *107*, 6257–6269.
- (97) Li, X.; Paldus, J. Truncated version of the reduced multireference coupled-cluster method with perturbation selection of higher than pair clusters. *International Journal of Quantum Chemistry* **2000**, *80*, 743–756.
- (98) Li, X.; Paldus, J. Reduced multireference coupled cluster method with singles and doubles: Perturbative corrections for triples. *The Journal of Chemical Physics* **2006**, *124*, 174101.
- (99) Li, X.; Paldus, J. Dissociation of N₂ triple bond: a reduced multireference CCSD study. *Chemical physics letters* **1998**, *286*, 145–154.
- (100) Li, X.; Paldus, J. Singlet-triplet splitting in methylene: An accurate description of dynamic and nondynamic correlation by reduced multireference coupled cluster method. *Collection of Czechoslovak chemical communications* **1998**, *63*, 1381–1393.

- (101) Li, X.; Paldus, J. Simultaneous handling of dynamical and nondynamical correlation via reduced multireference coupled cluster method: Geometry and harmonic force field of ozone. *The Journal of chemical physics* **1999**, *110*, 2844–2852.
- (102) Li, X.; Paldus, J. Reduced multireference coupled cluster method: Ro-vibrational spectra of N₂. *The Journal of Chemical Physics* **2000**, *113*, 9966–9977.
- (103) Li, X.; Paldus, J. Effect of spin contamination on the prediction of barrier heights by coupled-cluster theory: F + H₂ → HF + H reaction. *International Journal of Quantum Chemistry* **2000**, *77*, 281–290.
- (104) Li, X.; Paldus, J. A truncated version of reduced multireference coupled-cluster method with singles and doubles and noniterative triples: Application to F₂ and Ni(CO)_n (n = 1, 2, and 4). *The Journal of chemical physics* **2006**, *125*, 164107.
- (105) Li, X.; Paldus, J. Singlet–triplet separation in BN and C₂: simple yet exceptional systems for advanced correlated methods. *Chemical physics letters* **2006**, *431*, 179–184.
- (106) Li, X.; Paldus, J. Reduced multireference coupled-cluster method: Barrier heights for heavy atom transfer, nucleophilic substitution, association, and unimolecular reactions. *The Journal of Physical Chemistry A* **2007**, *111*, 11189–11197.
- (107) Li, X.; Paldus, J. Coupled-cluster approach to spontaneous symmetry breaking in molecules: The linear N₃ radical. *International Journal of Quantum Chemistry* **2008**, *108*, 2117–2127.
- (108) Li, X.; Paldus, J. Full potential energy curve for N₂ by the reduced multireference coupled-cluster method. *The Journal of Chemical Physics* **2008**, *129*, 054104.
- (109) Kowalski, K.; Piecuch, P. The method of moments of coupled-cluster equations and the renormalized CCSD[T], CCSD(T), CCSD(TQ), and CCSDT(Q) approaches. *J. Chem. Phys.* **2000**, *113*, 18.

- (110) Dunning, T. H. Gaussian basis sets for use in correlated molecular calculations. I. The atoms boron through neon and hydrogen. *J. Chem. Phys.* **1989**, *90*, 1007–1023.
- (111) Sun, Q.; Berkelbach, T. C.; Blunt, N. S.; Booth, G. H.; Guo, S.; Li, Z.; Liu, J.; McClain, J. D.; Sayfutyarova, E. R.; Sharma, S.; Wouters, S.; Chan, G. K. PySCF: the Python-based simulations of chemistry framework. 2017; <https://onlinelibrary.wiley.com/doi/abs/10.1002/wcms.1340>.
- (112) Chan, G. K.-L.; Head-Gordon, M. Highly correlated calculations with a polynomial cost algorithm: A study of the density matrix renormalization group. *The Journal of Chemical Physics* **2002**, *116*, 4462–4476.
- (113) Chan, G. K.-L. An algorithm for large scale density matrix renormalization group calculations. *The Journal of Chemical Physics* **2004**, *120*, 3172–3178.
- (114) Ghosh, D.; Hachmann, J.; Yanai, T.; Chan, G. K.-L. Orbital optimization in the density matrix renormalization group, with applications to polyenes and \hat{I}^2 -carotene. *The Journal of Chemical Physics* **2008**, *128*, 144117.
- (115) Sharma, S.; Chan, G. K.-L. Spin-adapted density matrix renormalization group algorithms for quantum chemistry. *The Journal of Chemical Physics* **2012**, *136*, 124121.
- (116) Sharma, S.; Holmes, A. A.; Jeanmairet, G.; Alavi, A.; Umrigar, C. J. Semistochastic Heat-Bath Configuration Interaction Method: Selected Configuration Interaction with Semistochastic Perturbation Theory. *J. Chem. Theory Comput.* **2017**, *13*, 1595–1604.
- (117) Holmes, A. A.; Tubman, N. M.; Umrigar, C. J. Heat-bath Configuration Interaction: An efficient selected CI algorithm inspired by heat-bath sampling. *J. Chem. Theory Comput.* **2016**, *12*, 3674–3680.
- (118) Smith, J. E. T.; Mussard, B.; Holmes, A. A.; Sharma, S. Cheap and Near Exact CASSCF

with Large Active Spaces. *Journal of Chemical Theory and Computation* **2017**, *13*, 5468–5478.

- (119) Nielsen, I. M. B.; Janssen, C. L. Double-substitution-based diagnostics for coupled-cluster and Møller–Plesset perturbation theory. *Chemical physics letters* **1999**, *310*, 568–576.
- (120) Magoulas, I.; Gururangan, K.; Piecuch, P.; Deustua, J. E.; Shen, J. Is Externally Corrected Coupled Cluster Always Better than the Underlying Truncated Configuration Interaction? 2021.

Appendix

A A sweep algorithm converting MPS to CI coefficients with a threshold

In DMRG, the electronic wave function is represented by a matrix-product state (MPS)

$$|\Psi\rangle = \sum_{n_1, \dots, n_K} \sum_{\alpha_1, \dots, \alpha_{K-1}} A_{\alpha_1}^{n_1} A_{\alpha_1 \alpha_2}^{n_2} \cdots A_{\alpha_{K-1}}^{n_K} |n_1 n_2 \cdots n_K\rangle, \quad (\text{A.1})$$

$$\{n\} = \{\text{vac}, \uparrow, \downarrow, \uparrow\downarrow\}, \quad (\text{A.2})$$

where n_i is the occupation of orbital i , $|n_1 n_2 \cdots n_K\rangle$ is the occupation-number representation of a determinant, and α_i is an auxiliary index. Here, $\sum_{\alpha_i} A_{\alpha_{i-1} \alpha_i}^{n_i} A_{\alpha_i \alpha_{i+1}}^{n_{i+1}}$ denotes a matrix product and it is assumed that the dimensions of all the auxiliary indices are the same (the bond dimension M). The wave function of the ground state can be optimized by the efficient DMRG sweep algorithm.

In order to get $Q_3^{\text{ec}}T_3$ and $Q_4^{\text{ec}}T_4$ in Eq. (2), we extract quadruple- and lower-order CI excitation amplitudes from the MPS by a sweep algorithm. To avoid repeated or unnecessary computation, we here describe how to obtain CI coefficients whose values are larger than a threshold in Eq. (3), with a concomitant reduction in computational cost and memory usage from a naive approach.

We first start with the MPS in left canonical form. During a sweep to compute the amplitude, at any given point (e.g. at some site p) one has a set of partial coefficients $c_{\alpha_p}(n_1 n_2 \dots n_p) = \sum_{\alpha_1 \dots \alpha_{p-1}} A_{\alpha_1}^{n_1} \dots A_{\alpha_{p-1} \alpha_p}^{n_p}$. If $\sum_{\alpha_p} |c_{\alpha_p}(n_1 n_2 \dots n_p)|^2 < \text{thresh}$, then this partial coefficient is dropped, as are all determinants involving the occupancy string $|n_1 n_2 \dots n_p\rangle$. This is because if the MPS is in left canonical form, the above condition on the partial coefficient guarantees that the coefficient of any determinant generated by the MPS which contains $|n_1 n_2 \dots n_p\rangle$ as a substring is also less than the threshold in magnitude. In addition, since the orbitals are associated with definite hole or particle character, we also drop any coefficient associated with more than 4 holes or 4 particles. Finally, in this process, we can take advantage of the conserved quantum numbers to

only generate symmetry unique partial coefficients (e.g. if $S_z = 0$, then the values of $c_{\alpha_{p+1}}$ come in time-reversal pairs and only one needs to be considered). Thus using the above algorithm we can completely avoid generating any determinants with coefficients below the threshold.